Author Manuscript

Author Manuscript

Author Manuscript

Author Manuscript

HHS Public Access

Author manuscript

Biomed Mater. Author manuscript; available in PMC 2021 October 03.

Published in final edited form as:

Biomed Mater. ; 15(6): 065017. doi:10.1088/1748-605X/aba40c.

Effect of sterilization treatment on mechanical properties, biodegradation, bioactivity and printability of GelMA hydrogels

Muhammad Rizwan[1], **Sarah W. Chan**[1], **Patricia A. Comeau**[2], **Thomas L. Willett**[2,3], **Evelyn K.F. Yim**[1,3,4]

[1]Department of Chemical Engineering, University of Waterloo, 200 University Avenue West, Waterloo, ON, Canada N2L 3G1

[2]Systems Design Engineering, University of Waterloo, 200 University Avenue West, Waterloo, ON, Canada N2L 3G1

[3]Centre for Biotechnology and Bioengineering, University of Waterloo, 200 University Avenue West, Waterloo, ON, Canada N2L 3G1

[4]Waterloo Institute for Nanotechnology, University of Waterloo, 200 University Avenue West, Waterloo, ON, Canada N2L 3G1

Abstract

Gelatin methacryloyl (GelMA) hydrogel scaffolds and GelMA-based bioinks are widely used in tissue engineering and bioprinting due to their ability to support cellular functions and new tissue development. Unfortunately, while terminal sterilization of the GelMA is a critical step for translational tissue engineering applications, it can potentially cause thermal or chemical modifications of GelMA. Thus, understanding the effect of terminal sterilization on GelMA properties is an important, though often overlooked, aspect of material design for translational tissue engineering applications. To this end, we characterized the effects of FDA-approved terminal sterilization methods (autoclaving, ethylene oxide treatment, and gamma (γ)-irradiation) on GelMA prepolymer (bioink) and GelMA hydrogels in terms of the relevant properties for biomedical applications, including mechanical strength, biodegradation rate, cell culture in 2D and 3D, and printability. Autoclaving and ethylene oxide treatment of the GelMA decreased the stiffness of the hydrogel, but the treatments did not modify the biodegradation rate of the hydrogel; meanwhile, γ-irradiation increased the stiffness, reduced the pore size and significantly slowed the biodegradation rate. None of the terminal sterilization methods changed the 2D fibroblast or endothelial cell adhesion and spreading. However, ethylene oxide treatment significantly lowered the fibroblast viability in 3D cell culture. Strikingly, γ-irradiation led to significantly reduced ability of the GelMA prepolymer to undergo sol-gel transition. Furthermore, printability studies showed that the bioinks prepared from γ-irradiated GelMA had significantly reduced printability as compared to the GelMA bioinks prepared from autoclaved or ethylene oxide treated GelMA. These results reveal that the choice of the terminal sterilization method can strongly influence important properties of GelMA bioink and hydrogel. Overall, this study provides further insight into GelMA-based material design with consideration of the effect of terminal sterilization.

*Corresponding author: Evelyn K.F. Yim, Department of Chemical Engineering, University of Waterloo, 200 University Avenue West, Waterloo, ON, Canada N2L 3G1, eyim@uwaterloo.ca.

Author Manuscript Author Manuscript Author Manuscript Author Manuscript

Keywords

GelMA; terminal sterilization; bioprinting; bioink; tissue engineering

Introduction

Gelatin methacryloyl (GelMA) hydrogels are widely used as scaffolds in tissue engineering due to their ability to support cellular functions and new tissue development by providing conducive cell-matrix interactions [1]. GelMA scaffolds contain naturally present cell adhesive ligands, and the biomechanical characteristics of the GelMA hydrogel can be fine-tuned with high precision by varying macromer concentration, UV crosslinking parameters, and through the application of facile sequential crosslinking [2]. GelMA prepolymer is also one of the most commonly used bioinks for 3D bioprinting due to tunable printability and favorable cellular adhesion properties [3–5]. Careful design principles are employed to impart specific characteristics (such as stiffness, bioactivity, biodegradation, 3D printability) in GelMA biomaterials for targeted tissue engineering applications [6–9]. Ideally, the sterilization treatment should not alter the carefully-designed biomechanical and biochemical properties of the GelMA prepolymer and scaffolds, ensuring that the scaffolds perform as intended after sterilization [10, 11]. This requirement renders the sterilization of the GelMA scaffolds a formidable task, as the hydrogels are more sensitive and prone to undergo chemical modifications during terminal sterilization process. Filtration is one of the commonly used methods of sterilization; however, as the concentration and/or the molecular weight of the biopolymer increase, filtration becomes gradually more difficult. Therefore, for different applications, other methods of sterilization are under investigation for biopolymers. Unfortunately, limited attention has been paid to the characterization of the effects of terminal sterilization on the GelMA prepolymer and scaffold properties. Work done by O'Connell and colleagues characterized the effects of sterilization on gelatin and GelMA, however this was mostly limited to rheological investigation of the bioinks [12]. In this study, we aimed to perform an in-depth analysis of the effects of various FDA-approved terminal sterilization techniques such as heat-based sterilization, ethylene oxide (EtO) treatment, and gamma irradiation (γ-irradiation) on the properties of GelMA prepolymer and hydrogel scaffolds.

Previous research has shown that terminal sterilization techniques may modify hydrogel properties. For example, heat-based sterilization such as autoclaving has good penetrability to allow for complete sterilization [10]. However, this sterilization approach can cause structural changes and degradation of hydrogels commonly used in tissue engineering [13, 14]. EtO treatment, which is another terminal sterilization technique, induces irreversible alkylation of cellular components; this effectively supresses metabolism and division of microorganisms or biological agent [10, 15]. In addition, studies have shown that EtO treatment can accelerate polymer degradation, leaving toxic residues and altering mechanical properties [16–20]. For example, Hooper *et al.* found that the EtO treatment could decrease yield strength and increase biodegradation rate of tyrosine-derived polycarbonates [16]. A further study observed that EtO treated and drug-loaded PLGA scaffolds had minimal burst release compared to the untreated scaffolds, which could also be

Author Manuscript Author Manuscript Author Manuscript Author Manuscript

linked to the microstructures changes of the PLGA scaffolds as a result of EtO treatment [21]. γ-irradiation offers another promising hydrogel sterilization method as it can sterilize the hydrogels at a relatively lower temperature in shorter duration compared to autoclaving and EtO treatment. It is known to have high penetration, the ability to break down DNA and RNA and to create reactive oxygen species (ROS) that can damage cellular components [10, 22, 23]. However, at the recommended dose of 25 kGy, γ-radiation can cause scission of polymer chains, which may lead to the reduction in polymer elastic modulus [24–26]. Additionally, γ-radiation is known to create chemical crosslinks in the solution phase of biomaterials, thus inducing sol-gel transition [27–29]. γ radiation has also been shown to induce crosslinking in gelatin solution [30, 31]. These studies emphasize the importance of studying the effects of the sterilization methods on GelMA properties, which could ultimately affect cellular adhesion, growth, and differentiation in GelMA scaffolds. In recent years, rheological properties of the hydrogel precursor solutions have gained tremendous importance due to their effect on printability of the hydrogel. Therefore, the effects of sterilization on the properties and printability of the GelMA prepolymer are critically important, yet unstudied to date.

To this end, we characterized the effects of terminal sterilization methods (autoclaving, EtO treatment, and γ-irradiation) on the relevant properties of GelMA for biomedical applications such as mechanical strength, biodegradation rate, cell culture in 2D and 3D GelMA scaffold, and printability.

2. Experimental details

2.1. Synthesis of gelatin methacryloyl hydrogels

Gelatin methacryloyl (GelMA) was synthesized as described previously [2]. Briefly, 10 g gelatin Type A, (Sigma-Aldrich) was dissolved in 100 mL 1X Phosphate Buffer Saline (PBS). 20 mL methacrylic anhydride (Sigma-Aldrich) was then added slowly to the 50 – 60 °C gelatin solution, before allowing the reaction to stir for an additional hour. Subsequently, the mixture was added to 12–14 kDa MWCO dialysis tubes and dialyzed in deionized water for 5 days at 37 °C. After dialysis, the GelMA monomer was frozen at −80 °C and lyophilized to obtain GelMA powder. The degree of methacrylation of gelatin was ≈94% as determined by using the 2,4,6-Trinitrobenzene Sulfonic Acid (TNBSA) assay [2].

2.2. Fabrication of gelatin methacryloyl hydrogels

To make the GelMA hydrogels, the GelMA powder was dissolved in 0.5% w/v Irgacure 2959 (BASF Inc) in 1X PBS at 50 °C at concentration range of 5% – 15% w/v to prepare a prepolymer solution. The solution was placed between glass slides to prepare GelMA films of different thicknesses, depending on the experiment performed. Subsequently, the solution was crosslinked with 365 nm UV light in HTBX UVLED curing oven (Height-LED Opto-electronics Tech Co) for 60 sec at 60 mW/cm^2.

Author Manuscript Author Manuscript Author Manuscript Author Manuscript

2.3. Sterilization of GelMA

GelMA was sterilized by using autoclaving, ethylene oxide (EtO) treatment or gamma (γ) irradiation at freeze-dried powder stage [Stage 1 (S1)] or at UV-crosslinked hydrogel stage [Stage 2 (S2)] (Fig. 1a).

Autoclaving: The GelMA powder was placed in an unvented glass bottle and autoclaved at 121 °C for 20 min to produce Stage-1 sterilized GelMA powder. The powder was then dissolved in an aqueous solution of photoinitiator and crosslinked as described in Section 2.2 to obtain stage-1-autoclaved GelMA hydrogel (A-GelMA^{S1}). To obtain stage-2-autoclaved GelMA hydrogels (A-GelMA^{S2}), untreated GelMA powder was used to cast untreated GelMA hydrogel, which was then incubated in excess DI water within a vented glass bottle and autoclaved at 121 °C for 20 min.

EtO treatment: The GelMA powder was sterilized by exposure to ethylene oxide gas (3M™ 8XL). The GelMA powder was preconditioned for 90 min at 55 °C and 70% relative humidity. Samples were then sterilized for 60 min with an EtO concentration of 759 mg/L at a pressure of 400–650 mbar. Pump down and purging was done for 60 min and the samples were aerated at 55 °C for 12 hrs. EtO treated GelMA powder was then converted to GelMA hydrogel, as described in Section 2.2, to obtain stage-1-EtO treated GelMA hydrogel (E-GelMA^{S1}). Stage-2-EtO treatment was not conducted on GelMA hydrogels, as the prerequisite of dehydrating the hydrogel for EtO treatment is known to change hydrogel properties [32, 33].

γ irradiation: The γ-sterilization was conducted by using γ-radiation produced with a Co-60 source (G.C. 220) at a dose of 25 kGy. The dose rate was calculated based on the half-life of the Co-60 source and the sterilization process was approximately 3790 min. The freeze dried GelMA powder was directly irradiated with γ-radiation to produce stage-1-irradiated GelMA powder. The powder was then converted to GelMA hydrogels, as described in Section 2.2, to obtain stage-1-irradiated GelMA hydrogels (γ-GelMA^{S1}). To obtain stage-2-irradiated GelMA hydrogels, untreated GelMA powder was used to obtain GelMA hydrogels which were then γ-irradiated to obtain γ-GelMA^{S2}.

In all of the stage-2 sterilizations, the samples were submerged in 1X PBS during the sterilization. The control samples (0.2 μm sterile-filtered) were also incubated in 1X PBS for the same amount of time prior to use in experiments.

2.4. Mechanical properties

Young's Modulus was measured on 15% w/v autoclaved (A-GelMA^{S1}; A-GelMA^{S2}), EtO-treated (E-GelMA^{S1}) and γ-irradiated (γ-GelMA^{S1}) hydrogels. 0.2 μm sterile filtered 15% w/v GelMA hydrogel was used as control. GelMA hydrogels of 8 mm diameter × 500 μm thickness were assessed for their Young's Modulus by using a Universal Mechanical Tester (UNMT-2MT, T1377, Center for Tribology, Inc.) with a 100N load cell and a constant compression rate of 10 μm/s. The data were plotted as a compressive stress-strain curve and the compressive Young's modulus was calculated as the slope of the linear region of the stress-strain curve corresponding to 0%–15% strain.

Author Manuscript Author Manuscript Author Manuscript Author Manuscript

2.5. Swelling analysis

To measure the effect of sterilization on swelling of the GelMA hydrogel, 15% prepolymer solutions were prepared and cast to form 500 μm thick × 6 mm diameter disks and lyophilized before recording the dry weight (Wd). Next, the hydrogels were re-hydrated in PBS buffer overnight at 37 °C and the swollen weights (Ws) were recorded. The percentage degree of swelling was measured as follows [34]:

$$\text{Degree of swelling } (\%) = [(Ws - Wd)/Wd] \times 100\%$$

We selected 15% w/v GelMA so that the samples are reasonably strong for handling and compressive modulus characterization. For the compressive modulus experiment, four replicates per group were used while three replicates per group were used for swelling analysis.

2.6. NMR analysis

To measure the NMR spectra, the 5% w/v prepolymer solutions were prepared in 90% D_2O:10% H_2O. The ^1H NMR spectra were obtained on a Bruker NMR 500 machine by using the pulse program. 128 scans were conducted with a relaxation time of 0.1 sec. to obtain the data. Estimation of the relative area under the methacryloyl vinyl peaks was used to calculate % methacryloyl groups left following sterilization using OriginPro 8.5 software. The data were then normalized to the untreated control group.

2.7. Pore size analysis

To analyze the pore size, hydrogel films with different sterilizations were frozen at −80 °C, freeze dried overnight, sputter coated, and then imaged with scanning electron microscope (Hitachi S-3500N) (SEM). The SEM images were analyzed in ImageJ, and the pore size was presented as the average of the maximum and minimum pore diameter of at least 50 pores per sample.

2.8. Biodegradation analysis

To characterize the effect of sterilization on the enzymatic cleavage of the GelMA hydrogels, samples of 8 mm diameter × 250 μm thickness were incubated in a 1 U/mL collagenase II enzyme (Sigma-Aldrich) solution for 7 days to measure the degradation rate. The enzyme solution was replaced daily to maintain the activity of the enzyme. A sample of 25 μL of the solution was taken at regular intervals and the biodegradation rate was measured by using BCA assay (Thermo Scientific), as per kit instructions, to measure the total protein release from the hydrogel due to biodegradation. Sterile-filtered samples were used as controls.

2.9. Rheological characterization of GelMA prepolymer

Sterile-filtered, autoclaved, EtO-treated and γ-irradiated GelMA powder was dissolved in 1X PBS overnight to prepare 10% w/v GelMA prepolymer solution for rheological measurements. Parallel plate geometry (20 mm) was used for dynamical rheological measurements in a Bohlin-CS Rheometer. The prepolymer solution was pipetted between

Author Manuscript Author Manuscript Author Manuscript Author Manuscript

the plates with a gap of 150 μm and temperature was lowered to 15 °C to induce physical gelation of the GelMA solution. The samples were kept at 15 °C for 10 min before the measurements were started. Dynamic storage (G') and loss modulus (G") were measured using a frequency sweep in 0.1 – 10 Hz frequency range at 1% strain to determine the response of the gels to varying frequency. The 1% strain was measured to be within the linear viscoelastic region.

The vial inversion test for sol-gel transition was performed on control and γ-GelMA[S1] samples. The vials were incubated at 4 °C for selected periods of time and the sol-gel transition was checked by inverting the vials.

2.10. 2D and 3D Cell attachment

Effect of sterilization methods on cellular attachment and spreading was characterized in 2D by seeding on the surface of 10% GelMA hydrogels and in 3D by cell encapsulation in 5% and 10% GelMA hydrogel. Primary human umbilical vein endothelial cells (HUVECs; Lonza) were cultured in Endothelial Cell Growth Medium (EGM-2, Lonza) with 2% fetal bovine serum (FBS), while primary human dermal fibroblasts cells (HDFs; Thermo Fisher Scientific) were cultured in Medium 106 supplemented with Low Serum Growth Supplement (LSGS; Thermo Fisher Scientific); both cell lines were maintained under standard cell culture conditions (37 °C, humidified, 5% CO_2 environment). Cells were passaged at 80–90% confluence using trypsin (Gibco) and seeded on GelMA films for experiments. GelMA hydrogel films made from 0.2 μm sterile filtered prepolymer solution were used as control. HUVECs and HDFs were seeded at 10,000 cells/cm^2 seeding density on GelMA films and cultured for 24 h before staining with Alexa Fluor™ 488 phalloidin (Life Technologies, 1:500 dilution) and 2 ng/mL of 4′,6-diamidino-2-phenylindole (DAPI, Sigma-Aldrich) for 30 min at room temperature. Subsequently, the cells were imaged with fluorescence microscope (ZEISS Axio Observer). The cell adhesion was analyzed by counting DAPI stained nuclei. For cell area analysis, the cell boundary was manually outlined and the area analyzed by using the "analyze particle" function provided by ImageJ.

For 3D cell encapsulation, HDFs were trypsinized and re-suspended in 5% and 10% GelMA prepolymer at a concentration of 2 million cells/ml. GelMA prepolymer solution were prepared from autoclaved, and EtO-treated freeze-dried GelMA powder with sterile-filtered 0.5% w/v photoinitiator solution. The cells were mixed in the prepolymer solutions, followed by UV-crosslinking for 60 sec in a 96-well plate. The cells were cultured for 7 days. Subsequently, they were analyzed with a Live/Dead cell viability assay by incubating for 60 min with 3.3 mM of calcein AM and 1.7 mM of ethidium homodimer-1 (Thermo Fisher Scientific). Subsequently, the cells in 3D hydrogels were imaged with a confocal microscope (ZEISS LSM 700). The cell viability was measured by counting the ratio of live (calcein stained; green) and dead (ethidium homodimer-1 stained; red) cells.

2.11. 3D printing of GelMA bioink

To measure the effect of sterilization on the printability of the GelMA bioink, GelMA solutions at a 10% w/v concentration were prepared with sterile-filtered GelMA as control. The GelMA bioink was then added to a 10 mL syringe (BD Luer-Lok™) with a ¼" long

Author Manuscript Author Manuscript Author Manuscript Author Manuscript

stainless-steel tip needle of gauge 27 (Nordson EFD) attached and allowed to cool for a minimum 30 min to room temperature under aluminum foil. A 3D grid pattern with the outer dimensions of 2 cm × 2 cm and line spacing of 4 mm was then printed using a System 30M 3D printer (Hyrel 3D) equipped with a SDS print head (Hyrel 3D) and a 385 nm PrimeCure™ light wand system (1 W/cm^2; Dymax®)[35]. Printing speed was set to 700 mm/min. ImageJ was used to measure the widths of the grid lines and determine the printability ratio, *Pr*, as per the following equation [36]:

$$Pr = L^2/16A$$

L is the perimeter of the interconnected channel and *A* is the area within the channel. In accordance with the above equation, perfect printability requires that the interconnected channels of the grid constructs demonstrate a square shape and have a *Pr* value of 1. Note that a square will have a consistent 4-sided length ("X"), a perimeter (*L*) of 4X and an area (*A*) of X^2. Entering these values into the above equation gives a *Pr* of 1. An acceptable printability ratio (*Pr*) range of 0.9 to 1.1 is typically reported in literature [36]. Incomplete grids were given a *Pr* of 0.

2.12. Statistical analysis

All data are presented as mean ± one standard deviation (SD). To determine the statistical significance of multiple comparisons one-way ANOVA with a Tukey's *post hoc* test was conducted with GraphPad Prism software for all characterization except printability. For printability, the same tests were conducted using IBM SPSS software. The sample number (n) is indicated in the figure captions for each experiment. The statistical significance threshold was set at $p \leq 0.05$.

3. Results

3.1. Effect of sterilization treatments on the compressive modulus of the GelMA

Compressive Young's modulus was measured on 15% GelMA hydrogels sterilized by autoclaving or ethylene oxide (EtO) treatment at Stage-1 (A-GelMA^{S1} and E-GelMA^{S1}), or autoclaving or γ-irradiation at Stage-2 (A-GelMA^{S2}, γ-GelMA^{S2}) (Fig. 1a). Untreated GelMA was used as control for both sets. The compressive moduli of A-GelMA^{S1} (16.5 kPa) and A-GelMA^{S2} (16.2 kPa) were significantly lower compared to control GelMA (28.7 kPa) (Fig. 1b). Similarly, compressive modulus of E-GelMA^{S1} (14.4 kPa) was also significantly lower compared to control ($P < 0.0001$) (Fig. 1b). However, compressive modulus of γ-GelMA^{S2} (39.7 kPa) was significantly higher compared to control ($P<0.001$) (Fig. 1b). No significant differences were found between the compressive modulus of A-GelMA^{S1}, A-GelMA^{S2}, and E-GelMA^{S1}.

3.2. Effect of sterilization treatments on the swelling of the GelMA

The swelling rate of the 15% GelMA hydrogels was measured by comparing the dry weight and swollen weight of the hydrogels in PBS buffer. The equilibrium swellings of A-GelMA^{S1} ($P < 0.05$), A-GelMA^{S2} ($P < 0.0001$), and E-GelMA^{S1} ($P < 0.001$), were significantly higher compared to control GelMA (Fig. 1c). Conversely, γ-GelMA^{S2} swelled

Author Manuscript Author Manuscript Author Manuscript Author Manuscript

significantly less compared to control (P<0.05), A-GelMA^{S1} (P<0.001), A-GelMA^{S2} (P<0.0001), and E-GelMA^{S1} (P<0.0001) (Fig. 1c). Interestingly, A-GelMA^{S2} swelled significantly more compared to A-GelMA^{S1} (P<0.05), which underlined the different effects of autoclaving at different stages of GelMA fabrication. The swellings of A-GelMA^{S1} and E-GelMA^{S1} were comparable.

3.3. Effect of sterilization treatments on the free methacryloyl groups in freeze dried GelMA macromers

Gross visual assessment showed that the γ-GelMA^{S1} formed significantly weaker gel (Fig. S1) compared to control GelMA. NMR analysis of the polymer after sterilization showed that the methacryloyl group peaks (specifically those at δ = 5.3 and 5.6 ppm, which represent the protons of the methacryloyl vinyl group of MA) in the γ-GelMA^{S1} were notably smaller compared to that of all other groups (Fig. 2a). Estimation of the area under the methacryloyl vinyl peaks showed that the percentage of methacryloyl groups left after sterilization were similar for the control, A-GelMA^{S1}, and E-GelMA^{S1}. However, methacryloyl groups present in γ-GelMA^{S1} drastically decreased (Fig. 2b). The change in hydrogel strength could be due to loss of methacryloyl groups on GelMA, which leads to insufficient crosslinking. The γ-GelMA^{S1} hydrogel was extremely weak and fragile, with a tendency to disintegrate when hydrated in PBS. Therefore, this sample group was omitted from further analysis.

3.4. Effect of sterilization treatments on the pore size and biodegradation rate of the GelMA hydrogel

Since γ-GelMA^{S2} gels were significantly stiffer, we hypothesized that the γ-GelMA^{S2} gels have increased crosslinking, which should result in smaller pore size. To test this hypothesis, we looked at the pore size of these gels. Indeed, pore size in γ-GelMA^{S2} gels was significantly smaller compared to all other groups (Fig. 3a,b and Fig. S2). The pore sizes of A-GelMA^{S1}, A-GelMA^{S2} and E-GelMA^{S1} were comparable to control GelMA. Pore size of E-GelMA^{S1} was significantly larger than A-GelMA^{S1}. GelMA hydrogels are known to be degraded by collagenase enzymatic cleavage [2]. We measured the biodegradation rate of the GelMA hydrogels with various sterilization treatments in collagenase II enzyme by quantifying the protein (gelatin) release in the solution. The biodegradation rates of the autoclaved hydrogels (A-GelMA^{S1} and A-GelMA^{S2}) were comparable to the control GelMA regardless of the stage of autoclaving (Fig. 3c). Similarly, the biodegradation rate of E-GelMA^{S1} was comparable to the control GelMA. All of these hydrogels completely degraded in about 48 hours. Strikingly, γ-GelMA^{S2} only degraded to about 33% in 48 hrs and took as much as 7 days to fully degraded (Fig. 3c). This indicated that the γ-irradiation process considerably slowed the biodegradation of the GelMA, which could be due to increased crosslinking in γ-GelMA^{S2} leading to smaller pore size, thereby requiring more cleavage activity to release the protein. Pore size and biodegradation are important parameters of hydrogels for 3D cell culture. GelMA hydrogels are often investigated at 5–10% concentration for improved cellular functions in 3D culture [37, 38]. Therefore, we lowered the GelMA concentration to 10% for pore size and biodegradation analysis, as well as for subsequent cell assays.

Author Manuscript Author Manuscript Author Manuscript Author Manuscript

3.5. Effect of GelMA hydrogel sterilization treatments on the 2D cell adhesion and spreading

The effect of sterilization on the bioactivity of the 10% GelMA hydrogel was analyzed by studying cellular adhesion and spreading of the human dermal fibroblasts (HDFs) and human umbilical vascular endothelial cells (HUVECs) on the GelMA surface (Fig. 4). The HDFs spread well on GelMA regardless of the sterilization treatment, which indicated a good cell matrix interaction (Fig. 4a). Quantitively, no significant differences were found in the adhesion or spreading of the HDFs (Fig. 4b and 4c). HUVECs also spread well on the GelMA regardless of the sterilization method used (Fig. 4d). There were no significant differences in the cell spreading area when analyzed quantitively (Fig. 4e). HUVEC attachment was higher on A-GelMA^{S1}, A-GelMA^{S2} and E-GelMA^{S1} compared to controls; however, the difference was not statistically detectable (Fig. 4f).

3.6. Effect of sterilization treatments on the sol-gel transition of the GelMA prepolymer

Physical gelation profoundly affects the mechanical properties and biodegradation of gelatin and the GelMA precursor [2]. The vial inversion test for sol-gel transition showed that the physical gelation behavior of γ-GelMA^{S1} was notably different as it failed to form a physical gel when it was incubated at 4 °C for 10 min (Fig. 5a). However, the control GelMA group readily transformed to gel state after 10 min. The γ-GelMA^{S1} took as much as 20 min to form a physical crosslinked gel (Fig. 5a). Gelatin as well as GelMA prepolymer are well known to form a physical gel at temperatures below 37 °C. Therefore, we further characterized the effect of sterilization on the physical gelation of the 10% GelMA prepolymer by using rheometry. We performed the rheological characterization on the prepolymer solution (instead of UV crosslinked hydrogels) because we were interested in understanding how sterilization would affect the rheological properties of the GelMA prepolymer, which are important for the bioprinting of GelMA prepolymer. The frequency sweep experiment from 0.1 – 10 Hz showed that the storage modulus (G') was significantly higher than the loss modulus (G") for GelMA, A-GelMA^{S1} and E-GelMA^{S1} prepolymer samples, which indicated that the gelation point had been reached (Fig. 5b). However, in the case of γ-GelMA^{S1} the G' was lower than the G", which indicated that the sol-gel transition had not yet occurred. These results complemented the gross visual examination of the gelation of control and γ-GelMA^{S1}. This further confirmed that the physical gelation of γ-GelMA^{S1} was significantly affected by γ-irradiation.

3.7. Effect of sterilization treatments on the viability of the encapsulated cells

We investigated the cellular response in 3D by encapsulating HDFs in A-GelMA^{S1} and E-GelMA^{S1} prepared at either 5 or 10% concentration. The γ-GelMA^{S1} was not included for cell encapsulation because the gels were extremely weak and unstable in PBS as explained in section 3.1. Fig. 6a shows the HDFs after 7-day encapsulation in control GelMA, E-GelMA^{S1} and A-GelMA^{S1}. The cell viability was slightly higher in 5% hydrogels compared to 10% hydrogels (Fig. 6b and 6c). In 5% GelMA hydrogels, the cell viability in E-GelMA^{S1} was significantly lower compared to the control GelMA ($p<0.05$), and slightly lower compared to A-GelMA^{S1} ($p=0.13$) (Fig. 6b). A similar trend was seen in 10% hydrogels as well, with lower cell viability found on E-GelMA^{S1} compared to control or A-

Author Manuscript Author Manuscript Author Manuscript Author Manuscript

GelMA[S1]; however, the results were not statistically significant in either case (Fig. 6b). Overall, cell viability in 3D conditions indicated that the type of sterilization method could affect the cell properties in 3D hydrogels. Therefore, it is critical to consider sterilization strategy to reduce any harmful effects on cell survival.

3.8. Effect of sterilization treatments on the printability of the GelMA bioinks

Finally, we investigated the effect of different sterilization treatments on the printability of the 10% GelMA prepolymer, which is commonly used as a bioink [37]. For repeatable and effective printing, the extruded filament should lay down on the print bed in lines of consistent width and produce the desired profile. In this investigation, untreated GelMA, EtO treated GelMA, and autoclaved GelMA exhibited stable curing behaviours during printing of multi-grid squares, with comparable and acceptable printability ratios (Pr = 0.98 +/− 0.02, 1.00 +/− 0.02, and 0.99 +/− 0.03, respectively) (Fig. 7). However, γ-treated GelMA bioink did not extrude or cure adequately during printability assessment. In fact, the grids printed using γ-treated GelMA bioink were largely incomplete, with more than half lacking all four edges; the printability ratio was very poor for this bioink (Pr = 0.32 +/− 0.32). The line width of the grids printed using the γ-treated GelMA was the least consistent, as well as detectably lower than that measured for the untreated GelMA ($p = 0.001$). However, the reported line width for each ink was notably higher than that expected with a 27-gauge needle (inner diameter of 0.21 mm).

4. Discussion

Understanding the consequences of terminal sterilization of hydrogels and the resulting changes in the hydrogel properties, whether positive or negative, is an important aspect for translational tissue engineering applications. However, it is often overlooked in material design strategy. This study demonstrated that the biomechanical, rheological, and biodegradation properties of the gelatin methacryloyl (GelMA) scaffolds following sterilization are dependent on the type of sterilization treatment. The effect of sterilization on the GelMA has not been studied in-depth previously, even though it is one of the most widely used hydrogel scaffolds in tissue engineering that requires conducive cell-matrix interactions [1, 39–45].

Autoclaving is a commonly used strategy in tissue engineering labs and is readily accessible to most laboratories interested in developing biomaterials for tissue engineering. However, in this study, autoclaving at the stage of freeze-dried powder form of GelMA (A-GelMA[S1]) or at UV-crosslinked hydrogel form of GelMA (A-GelMA[S2]) lowered the compressive moduli of the hydrogels compared to untreated GelMA. Autoclaving is a high temperature process that has previously been shown to cause thermal degradation in polymers [13, 46]. Thermal degradation can also occur when autoclaving is performed on the biopolymers submerged in buffer [46, 47]. We speculate that the loss in stiffness could be attributed to the thermal degradation of the freeze-dried GelMA or GelMA hydrogels. Similarly, EtO treated GelMA (E-GelMA[S1]) had lower compressive modulus compared to untreated GelMA, which could also be a result of chain degradation due to EtO treatment; this has been described in earlier studies [19]. However, more studies, such as size exclusion

Author Manuscript Author Manuscript Author Manuscript Author Manuscript

chromatography, shall be conducted in the future to understand the effect of polymer degradation due to sterilization and its effect on mechanical behavior of GelMA hydrogels.

Meanwhile, gamma (γ) irradiation had inverse consequences on the stiffness of the GelMA depending on the stage of the treatment stage. The GelMA freeze dried polymer γ-irradiated at stage-1 could only form a very weak hydrogel. However, γ-irradiation at stage-2 (γ-GelMA^{S2}) resulted in significantly stiffer GelMA compared to untreated GelMA (Fig. 1b). Previous studies have shown that the γ-irradiation could cause additional crosslinking in the hydrogels [29, 31]. It is likely than that the increased compressive modulus in γ-GelMA^{S2} is a result of γ-mediated crosslinking of gelatin chains, as noted in a previous study [30]. Biodegradation is a crucial parameter that could affect cellular functions such as cell migration in 3D through enzymatic cleavage of the extracellular environment, as well as drug release from drug-loaded scaffolds. Autoclaving and EtO treatment did not alter biodegradation properties; however, the γ-GelMA^{S2} biodegraded significantly slower than the rest of the groups (Fig. 1c). The slower biodegradation rate could be a result of increased crosslinking and smaller pore size, which would in turn reduce the swelling of γ-GelMA^{S2} [2]. Subsequently, this limited swelling would reduce enzyme diffusion into the matrix to degrade the scaffold. Another possible reason could be the oxidative damage of the protein, thereby changing the target site of the collagenase. Crosslinking of the collagenase-sensitive peptide sequences of the gelatin could potentially occur due to gamma irradiation; this could in turn slow down the degradation process. Further studies need to be conducted to verify this potential side-effect of gamma irradiation. Interestingly, γ-GelMA^{S1} had completely different properties. The γ-GelMA^{S1} was extremely fragile and weak, and disintegrated in the PBS when stored overnight, which made it practically unusable as a tissue engineering scaffold. Loss of methacryloyl groups of the GelMA, as observed in the NMR data, and fewer vinyl groups available following γ-sterilization for UV polymerization could explain extremely fragile γ-GelMA^{S1} hydrogel that was formed upon UV exposure.

Previous studies have shown that gamma radiation produces free radicals [48]. Since the γ-GelMA^{S1} contains unreacted methacryloyl, we hypothesize that the generation of free radicals could initiate methacryloyl reaction with nearby methacryloyl moieties. This methacryloyl reaction could lead to a reduction in the available methacryloyl moieties for UV crosslinking of γ-GelMA^{S1} prepolymer. The result also highlights the importance of careful consideration of the stage at which GelMA hydrogel is sterilized.

We characterized the bioactivity of the GelMA hydrogels with different sterilization treatments by using two different types of primary cells in 2D and 3D. The human dermal fibroblast cells (HDFs) as well as human umbilical vein endothelial cells (HUVECs) surface attachment and density was comparable for untreated, autoclaved, EtO treated and γ-treated GelMA. The observations suggest that the cell adhesive RGD ligands representation is not affected by choice of the sterilization method. However, the cellular response was different when the cells were encapsulated in GelMA prepolymer solution prior to UV crosslinking. We chose Irgacure 2959 photoinitiator for UV curing of cell-laden GelMA because of its well-known cytocompatibility and applications in tissue engineering [1, 4, 39, 49]. A recent study has also demonstrated, with multiple cell types, that the exposure to low dose 365 nm wavelength UV light (such as the dose used in our study) does not induce changes in

Author Manuscript Author Manuscript Author Manuscript Author Manuscript

proliferation, apoptotic induction or proteome of the cells [50]. The 7-day HDF cell viability in A-GelMA^{S1} was similar to the untreated GelMA in 5% and 10% hydrogels, but it was significantly reduced in E-GelMA^{S1}. EtO treatment is known to leave toxic residues in the scaffolds [10]. The slower cell growth in E-GelMA^{S1} observed in this study could be due to the presence of toxic residues. Interestingly, the cellular adhesion and density was not significantly different when the cells were seeded on the surface of E-GelMA^{S1}. This could be due to the washing of the gels prior to cell seeding that removed the toxic residues. However, washing cannot be performed when the cells are encapsulated in the prepolymer. Therefore, such residue could have more deleterious effects in 3D culture of cells in EtO treated hydrogels compared to 2D culture. This highlights that the toxic effect of the sterilization treatment should be kept in mind when choosing a sterilization strategy, particularly for 3D cell culture. The selected duration of 3D cell culture study used is acceptable for long term 3D cell culture experiments. However, any remaining toxic products from the sterilization may better be cleared with an extended study time period. The selected end point may be a study limitation as the acute toxic effects of sterilization will need further appreciation. Future studies should be conducted to investigate shorter time point as well.

Physical gelation of the gelatin and GelMA solution is attributed to the partial reformation of the triple helical structures upon lowering the temperature below room temperature [2]. Non-covalent interactions between nearby chains, such as hydrogen bonding, hold the key for the formation of alpha helices. A recent study from our group showed the importance of physical gelation in GelMA prepolymer to produce stronger GelMA hydrogels through a sequential crosslinking approach (physical gelation followed by UV curing) [2]. The γ-GelMA^{S1} prepolymer took twice as much time compared to the control GelMA, E-GelMA^{S1} and A-GelMA^{S1} for sol-gel transition. The γ-irradiation seems to alter chemical structure of the GelMA molecules in such a way that the formation of triple helical structures is significantly slowed, leading to hampered sol-gel transition.

GelMA prepolymer (also known as GelMA bioink) is widely used for 3D printing for biofabrication of scalable and complex tissue engineering scaffolds. The rate at which GelMA prepolymer solution undergoes sol-gel transition will affect its rate of change of viscosity, which could affect the printability of the GelMA prepolymer [8, 49, 51, 52]. Following the printability assessment of the GelMA bioinks, it was readily apparent that EtO and autoclave treatments did not significantly alter the ability of the GelMA bioink to be printed. There was no detectable difference in the semi-quantitative measure of printability (ratio) for these three inks. However, γ-treated GelMA bioink led to a 3D-printed square lacking more than half of its 25 inner grids, and was given a poor printability ratio as a result. This latter ink was notably challenged with both inconsistent filament formation during extrusion and poor curing during 3D printing. Together these two behaviors contributed to the poor assessment of printability for this bioink. All inks exhibited some line collapse, as shown by an apparent increase in line width from that expected (based on needle diameter). However, some deviation from extruder needle diameter is common in literature and it is not necessarily considered a sign of a poorly designed ink. The results of the current study also emphasize that the effects of sterilization treatment on GelMA

Author Manuscript Author Manuscript Author Manuscript Author Manuscript

prepolymer should be taken into consideration for effective GelMA bioink design towards 3D bioprinting applications.

5. Conclusion

We characterized the effects of various terminal sterilization methods on the mechanical properties, biodegradation, bioactivity and printability of gelatin methacryloyl (GelMA) prepolymer and/or scaffolds. Autoclaving and EtO sterilization significantly reduced the compressive modulus of GelMA, while gamma irradiation (γ-irradiation) significantly increased this same property. γ-irradiation also reduced the pore size and biodegradation rate of the GelMA scaffolds, as well as significantly slowed the sol-gel transition of the GelMA prepolymer. This latter effect could be due to the reduced ability of the γ-irradiated GelMA polymer to form alpha helices. Remarkably, cell adhesion and spreading on 2D GelMA surface was not significantly affected by different sterilization techniques; however, EtO sterilization treatment reduced the viability of the encapsulated cells. Lastly, we showed that the γ-irradiation deteriorated the printability of the GelMA, which could be linked to the deleterious effect of γ-irradiation on sol-gel transition. This study emphasizes the importance of careful consideration of the stage at which GelMA should be sterilized. For instance, tissue engineering applications that require stiffer and slowly degradable GelMA matrices could benefit from γ-irradiation at stage-2. Taking all aspects into consideration, we believe that autoclaving presents a promising strategy for sterilization at Stage-1 and Stage-2 of GelMA, as it does not cause cytotoxic effects, mechanical properties are largely similar to sterile-filtered GelMA, and bioprintability is not affected.

Supplementary Material

Refer to Web version on PubMed Central for supplementary material.

Acknowledgments

This work was supported by the NSERC Canada Discovery Grant (RGPIN-2016-04043), University of Waterloo Startup Fund, and partially funded by National Institutes of Health (R01HL130274). SC received financial support from NSERC Canada Discovery Grant (RGPIN-2016-04043), NSERC USRA and Ontario Graduate Scholarship. TL Willett would like to thank the Canadian Institutes of Health Research (CIHR) (No. 389569) for research funding. The authors thank S. Mattiassi for proofreading this manuscript.

6. References

[1]. Yue K, Trujillo-de Santiago G, Alvarez MM, Tamayol A, Annabi N, Khademhosseini A, Synthesis, properties, and biomedical applications of gelatin methacryloyl (GelMA) hydrogels, Biomaterials 73 (2015) 254–71. [PubMed: 26414409]

[2]. Rizwan M, Peh GSL, Ang H-P, Lwin NC, Adnan K, Mehta JS, Tan WS, Yim EKF, Sequentially-crosslinked bioactive hydrogels as nano-patterned substrates with customizable stiffness and degradation for corneal tissue engineering applications, Biomaterials 120 (2017) 139–154. [PubMed: 28061402]

[3]. Xie M, Gao Q, Zhao H, Nie J, Fu Z, Wang H, Chen L, Shao L, Fu J, Chen Z, He Y, Electro-Assisted Bioprinting of Low-Concentration GelMA Microdroplets, Small 15(4) (2019).

[4]. Ying G, Jiang N, Yu C, Zhang YS, Three-dimensional bioprinting of gelatin methacryloyl (GelMA), Bio-Design and Manufacturing 1(4) (2018) 215–224.

Author Manuscript Author Manuscript Author Manuscript Author Manuscript

[5]. Yin J, Yan M, Wang Y, Fu J, Suo H, 3D Bioprinting of Low-Concentration Cell-Laden Gelatin Methacrylate (GelMA) Bioinks with a Two-Step Cross-linking Strategy, Acs Appl Mater Inter 10(8) (2018) 6849–6857.

[6]. El-Sherbiny IM, Yacoub MH, Hydrogel scaffolds for tissue engineering: Progress and challenges, Global cardiology science & practice 2013(3) (2013) 316–42. [PubMed: 24689032]

[7]. Zhu J, Marchant RE, Design properties of hydrogel tissue-engineering scaffolds, Expert review of medical devices 8(5) (2011) 607–26. [PubMed: 22026626]

[8]. Malda J, Visser J, Melchels FP, Jungst T, Hennink WE, Dhert WJ, Groll J, Hutmacher DW, 25th anniversary article: Engineering hydrogels for biofabrication, Adv Mater 25(36) (2013) 5011–28. [PubMed: 24038336]

[9]. Slaughter BV, Khurshid SS, Fisher OZ, Khademhosseini A, Peppas NA, Hydrogels in regenerative medicine, Adv Mater 21(32–33) (2009) 3307–29. [PubMed: 20882499]

[10]. Dai Z, Ronholm J, Tian Y, Sethi B, Cao X, Sterilization techniques for biodegradable scaffolds in tissue engineering applications, Journal of Tissue Engineering 7 (2016) 2041731416648810. [PubMed: 27247758]

[11]. Galante R, Pinto TJA, Colaço R, Serro AP, Sterilization of hydrogels for biomedical applications: A review, Journal of Biomedical Materials Research Part B: Applied Biomaterials 106(6) (2018) 2472–2492. [PubMed: 29247599]

[12]. O'Connell CD, Onofrillo C, Duchi S, Li X, Zhang Y, Tian P, Lu L, Trengove A, Quigley A, Gambhir S, Khansari A, Mladenovska T, O'Connor A, Di Bella C, Choong PF, Wallace GG, Evaluation of sterilisation methods for bio-ink components: gelatin, gelatin methacryloyl, hyaluronic acid and hyaluronic acid methacryloyl, Biofabrication 11(3) (2019) 035003. [PubMed: 30818298]

[13]. Zhang X, Takegoshi K, Hikichi K, Phase separation and thermal degradation of poly(vinyl alcohol)/poly(methacrylic acid) and poly(vinyl alcohol)/poly(acrylic acid) systems by 13C c.p./m.a.s. n.m.r, Polymer 33(4) (1992) 718–724.

[14]. Tsuchiya Y, Sumi K, Thermal decomposition products of poly(vinyl alcohol), Journal of Polymer Science Part A-1: Polymer Chemistry 7(11) (1969) 3151–3158.

[15]. Gogolewski S, Mainil-Varlet P, Effect of thermal treatment on sterility, molecular and mechanical properties of various polylactides. 2. Poly(L/D-lactide) and poly(L/DL-lactide), Biomaterials 18(3) (1997) 251–5. [PubMed: 9031727]

[16]. Hooper KA, Cox JD, Kohn J, Comparison of the effect of ethylene oxide and γ-irradiation on selected tyrosine-derived polycarbonates and poly(L-lactic acid), Journal of Applied Polymer Science 63(11) (1997) 1499–1510.

[17]. Volland C, Wolff M, Kissel T, The influence of terminal gamma-sterilization on captopril containing poly(d,l-lactide-co-glycolide) microspheres, J Control Release 31(3) (1994) 293–305.

[18]. Zislis T, Mark DE, Cerbas EL, Hollinger JO, Scanning electron microscopic study of cell attachment to biodegradable polymer implants, The Journal of oral implantology 15(3) (1989) 160–7. [PubMed: 2561760]

[19]. Holy CE, Cheng C, Davies JE, Shoichet MS, Optimizing the sterilization of PLGA scaffolds for use in tissue engineering, Biomaterials 22(1) (2000) 25–31.

[20]. Pohan G, Mattiassi S, Yao Y, Zaw AM, Anderson DEJ, Cutiongco MFA, Hinds MT, Yim EKF, Effect of ethylene oxide sterilization on polyvinyl alcohol hydrogel compared to gamma radiation, Tissue Eng Pt A 19-20 (2020) 1077–1090.

[21]. Hsiao C-Y, Liu S-J, Wen-Neng Ueng S, Chan E-C, The influence of γ irradiation and ethylene oxide treatment on the release characteristics of biodegradable poly(lactide-co-glycolide) composites, Polymer Degradation and Stability 97(5) (2012) 715–720.

[22]. Cox MM, Battista JR, Deinococcus radiodurans - the consummate survivor, Nature reviews. Microbiology 3(11) (2005) 882–92. [PubMed: 16261171]

[23]. Lambert PA, Radiation Sterilization, Russell, Hugo & Ayliffe's, Wiley-Blackwell2013, pp. 294–305.

[24]. Yunoki S, Ikoma T, Monkawa A, Ohta K, Tanaka J, Sotome S, Shinomiya K, Influence of γ Irradiation on the Mechanical Strength and In Vitro Biodegradation of Porous Hydroxyapatite/Collagen Composite, Journal of the American Ceramic Society 89(9) (2006) 2977–2979.

Author Manuscript Author Manuscript Author Manuscript Author Manuscript

[25]. Plikk P, Odelius K, Hakkarainen M, Albertsson AC, Finalizing the properties of porous scaffolds of aliphatic polyesters through radiation sterilization, Biomaterials 27(31) (2006) 5335–5347. [PubMed: 16846641]

[26]. Amadori S, Torricelli P, Rubini K, Fini M, Panzavolta S, Bigi A, Effect of sterilization and crosslinking on gelatin films, J Mater Sci Mater Med 26(2) (2015) 69. [PubMed: 25631265]

[27]. Valente TA, Silva DM, Gomes PS, Fernandes MH, Santos JD, Sencadas V, Effect of Sterilization Methods on Electrospun Poly(lactic acid) (PLA) Fiber Alignment for Biomedical Applications, ACS Appl Mater Interfaces 8(5) (2016) 3241–9. [PubMed: 26756809]

[28]. Clough RL, High-energy radiation and polymers: A review of commercial processes and emerging applications, Nuclear Instruments and Methods in Physics Research Section B: Beam Interactions with Materials and Atoms 185(1) (2001) 8–33.

[29]. Inoue N, Bessho M, Furuta M, Kojima T, Okuda S, Hara M, A novel collagen hydrogel cross-linked by gamma-ray irradiation in acidic pH conditions, J Biomat Sci-Polym E 17(8) (2006) 837–858.

[30]. Cataldo F, Ursini O, Lilla E, Angelini G, Radiation-induced crosslinking of collagen gelatin into a stable hydrogel, J Radioanal Nucl Ch 275(1) (2008) 125–131.

[31]. Islam MM, Khan MA, Rahman MM, Preparation of gelatin based porous biocomposite for bone tissue engineering and evaluation of gamma irradiation effect on its properties, Materials Science and Engineering C 49 (2015) 648–655. [PubMed: 25686994]

[32]. Thomas J, Gomes K, Lowman A, Marcolongo M, The effect of dehydration history on PVA/PVP hydrogels for nucleus pulposus replacement, J Biomed Mater Res B Appl Biomater 69(2) (2004) 135–40. [PubMed: 15116402]

[33]. Alam MM, Mina MF, Akhtar F, Swelling and Hydration Properties of Acrylamide Hydrogel in Distilled Water, Polymer-Plastics Technology and Engineering 42(4) (2003) 533–542.

[34]. Paciello A, Santonicola MG, Supramolecular polycationic hydrogels with high swelling capacity prepared by partial methacrylation of polyethyleneimine, RSC Advances 5(108) (2015) 88866–88875.

[35]. Comeau P, Willett T, Printability of Methacrylated Gelatin upon Inclusion of a Chloride Salt and Hydroxyapatite Nano-Particles, Macromolecular Materials and Engineering 304(8) (2019) 1900142.

[36]. Ouyang L, Yao R, Zhao Y, Sun W, Effect of bioink properties on printability and cell viability for 3D bioplotting of embryonic stem cells, Biofabrication 8(3) (2016) 035020. [PubMed: 27634915]

[37]. Bertassoni LE, Cardoso JC, Manoharan V, Cristino AL, Bhise NS, Araujo WA, Zorlutuna P, Vrana NE, Ghaemmaghami AM, Dokmeci MR, Khademhosseini A, Direct-write bioprinting of cell-laden methacrylated gelatin hydrogels, Biofabrication 6(2) (2014) 024105. [PubMed: 24695367]

[38]. Rastin H, Ormsby RT, Atkins GJ, Losic D, 3D Bioprinting of Methylcellulose/Gelatin-Methacryloyl (MC/GelMA) Bioink with High Shape Integrity, ACS Applied Bio Materials 3(3) (2020) 1815–1826.

[39]. Zhao X, Lang Q, Yildirimer L, Lin ZY, Cui W, Annabi N, Ng KW, Dokmeci MR, Ghaemmaghami AM, Khademhosseini A, Photocrosslinkable Gelatin Hydrogel for Epidermal Tissue Engineering, Adv Healthc Mater 5(1) (2016) 108–118. [PubMed: 25880725]

[40]. Nemeth CL, Janebodin K, Yuan AE, Dennis JE, Reyes M, Kim DH, Enhanced chondrogenic differentiation of dental pulp stem cells using nanopatterned PEG-GelMA-HA hydrogels, Tissue Engineering - Part A 20(21–22) (2014) 2817–2829. [PubMed: 24749806]

[41]. Levett PA, Melchels FPW, Schrobback K, Hutmacher DW, Malda J, Klein TJ, A biomimetic extracellular matrix for cartilage tissue engineering centered on photocurable gelatin, hyaluronic acid and chondroitin sulfate, Acta Biomaterialia 10(1) (2014) 214–223. [PubMed: 24140603]

[42]. Heo DN, Ko WK, Bae MS, Lee JB, Lee DW, Byun W, Lee CH, Kim EC, Jung BY, Kwon IK, Enhanced bone regeneration with a gold nanoparticle-hydrogel complex, J Mater Chem B 2(11) (2014) 1584–1593. [PubMed: 32261377]

Author Manuscript Author Manuscript Author Manuscript Author Manuscript

[43]. Ahadian S, Ramón-Azcón J, Estili M, Obregón R, Shiku H, Matsue T, Facile and rapid generation of 3D chemical gradients within hydrogels for high-throughput drug screening applications, Biosensors and Bioelectronics 59 (2014) 166–173. [PubMed: 24727602]

[44]. Zhu K, Shin SR, van Kempen T, Li YC, Ponraj V, Nasajpour A, Mandla S, Hu N, Liu X, Leijten J, Lin YD, Hussain MA, Zhang YS, Tamayol A, Khademhosseini A, Gold Nanocomposite Bioink for Printing 3D Cardiac Constructs, Adv Funct Mater 27(12) (2017).

[45]. Navaei A, Saini H, Christenson W, Sullivan RT, Ros R, Nikkhah M, Gold nanorod-incorporated gelatin-based conductive hydrogels for engineering cardiac tissue constructs, Acta Biomater 41 (2016) 133–46. [PubMed: 27212425]

[46]. van den Bosch E, Gielens C, Gelatin degradation at elevated temperature, International journal of biological macromolecules 32(3–5) (2003) 129–38. [PubMed: 12957309]

[47]. Kunioka M, Choi HJ, Hydrolytic degradation and mechanical properties of hydrogels prepared from microbial poly(amino acid)s, Polymer Degradation and Stability 59(1) (1998) 33–37.

[48]. Rajeswara Rao N, Venkatappa Rao T, Ramana Reddy SVS, Sanjeeva Rao B, The effect of gamma irradiation on physical, thermal and antioxidant properties of kraft lignin, Journal of Radiation Research and Applied Sciences 8(4) (2015) 621–629.

[49]. Pepelanova I, Kruppa K, Scheper T, Lavrentieva A, Gelatin-Methacryloyl (GelMA) Hydrogels with Defined Degree of Functionalization as a Versatile Toolkit for 3D Cell Culture and Extrusion Bioprinting, Bioengineering (Basel) 5(3) (2018) 55.

[50]. Ruskowitz ER, DeForest CA, Proteome-wide Analysis of Cellular Response to Ultraviolet Light for Biomaterial Synthesis and Modification, ACS Biomaterials Science & Engineering 5(5) (2019) 2111–2116.

[51]. Gungor-Ozkerim PS, Inci I, Zhang YS, Khademhosseini A, Dokmeci MR, Bioinks for 3D bioprinting: an overview, Biomater Sci 6(5) (2018) 915–946. [PubMed: 29492503]

[52]. Kiyotake EA, Douglas AW, Thomas EE, Nimmo SL, Detamore MS, Development and quantitative characterization of the precursor rheology of hyaluronic acid hydrogels for bioprinting, Acta Biomaterialia 95 (2019) 176–87. [PubMed: 30669003]

Author Manuscript Author Manuscript Author Manuscript Author Manuscript

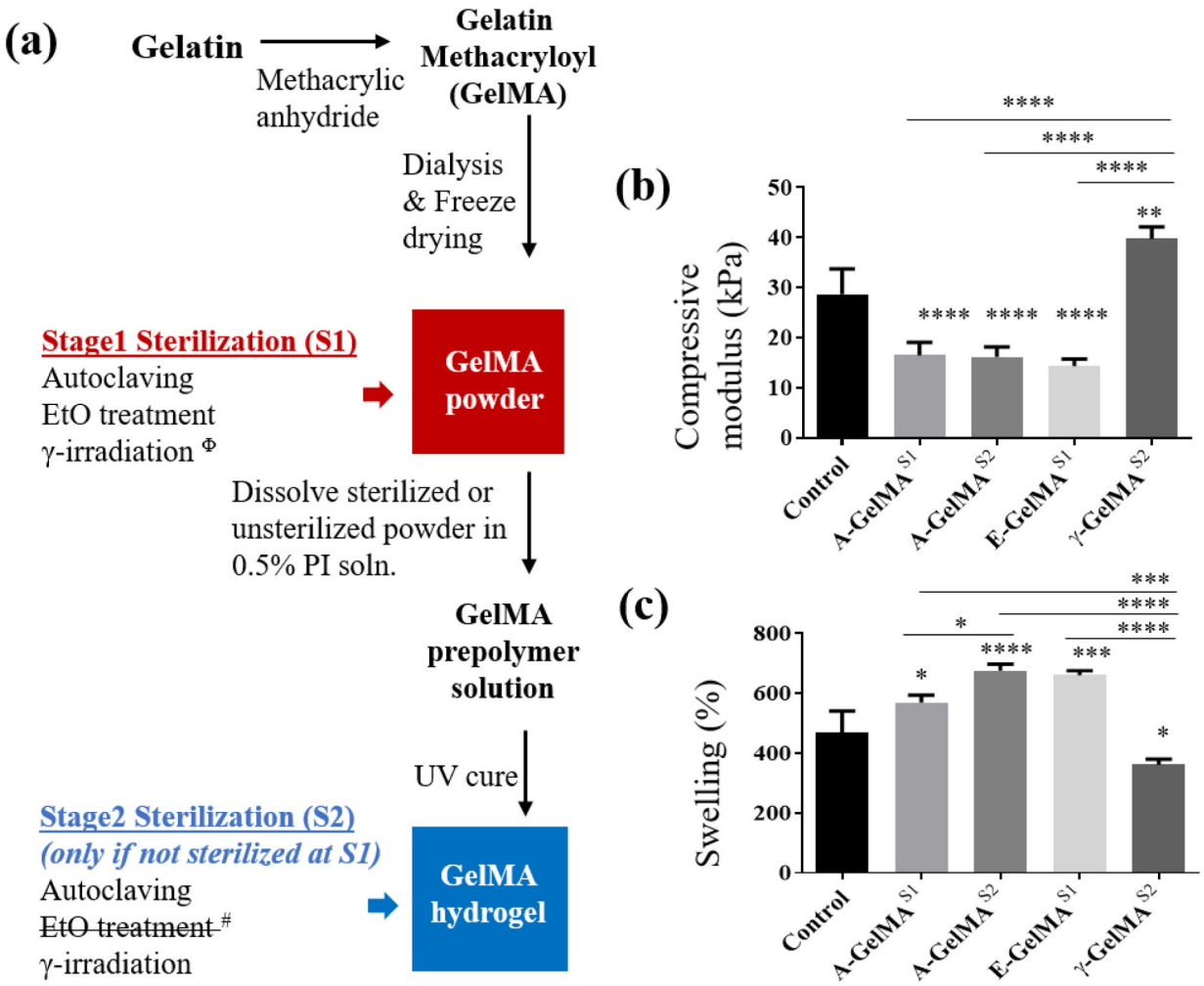

Figure 1:

(a) Explanation of the GelMA preparation and sterilization at different stages. Effect of sterilization on 15% GelMA (b) compressive modulus and (c) swelling. Φ Gamma irradiated GelMA powder did not form a hydrogel when dissolved in photo initiator solution and exposed to UV. # EtO treatment at S2 stage is incompatible due the presence of water in hydrogels. Control = sterile filtered GelMA; A-GelMA^{S1} = GelMA autoclaved at stage 1; A-GelMA^{S2} = GelMA autoclaved at stage 2; E-GelMA^{S1} = GelMA sterilized with ethylene oxide at stage 1; γ-GelMA^{S2} = GelMA gamma irradiated at stage 2. * $p<0.05$; ** $p<0.01$; *** $p<0.001$; **** $p<0.0001$. n=4 for (b). n=3 for (c).

Author Manuscript Author Manuscript Author Manuscript Author Manuscript

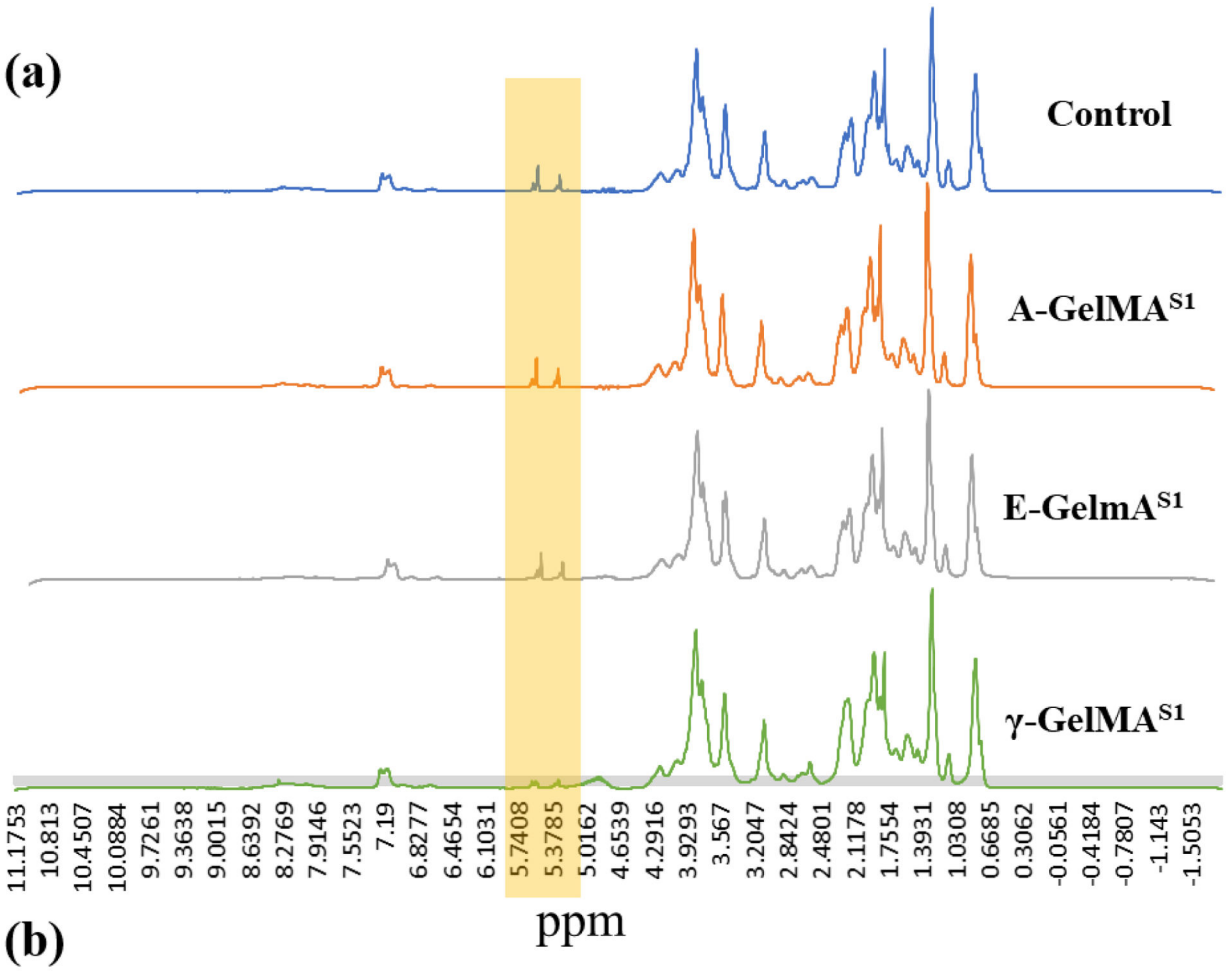

(b)

% methacryloyl groups left after sterilization (normalized)

Control	A-GelMAS1	E-GelMAS1	γ-GelMAS1
100	101.5	95.1	29.8

Figure 2:

(**a**) NMR showing the smaller peak of methacryloyl groups (The signal at δ = 5.3 and 5.6 ppm) on the GelMA after gamma sterilization at stage 1 compared to rest of the groups. (b) Relative area under the peak estimation to calculate the % methacryloyl groups left after sterilization. The data was normalized to the untreated control group.

Author Manuscript Author Manuscript Author Manuscript Author Manuscript

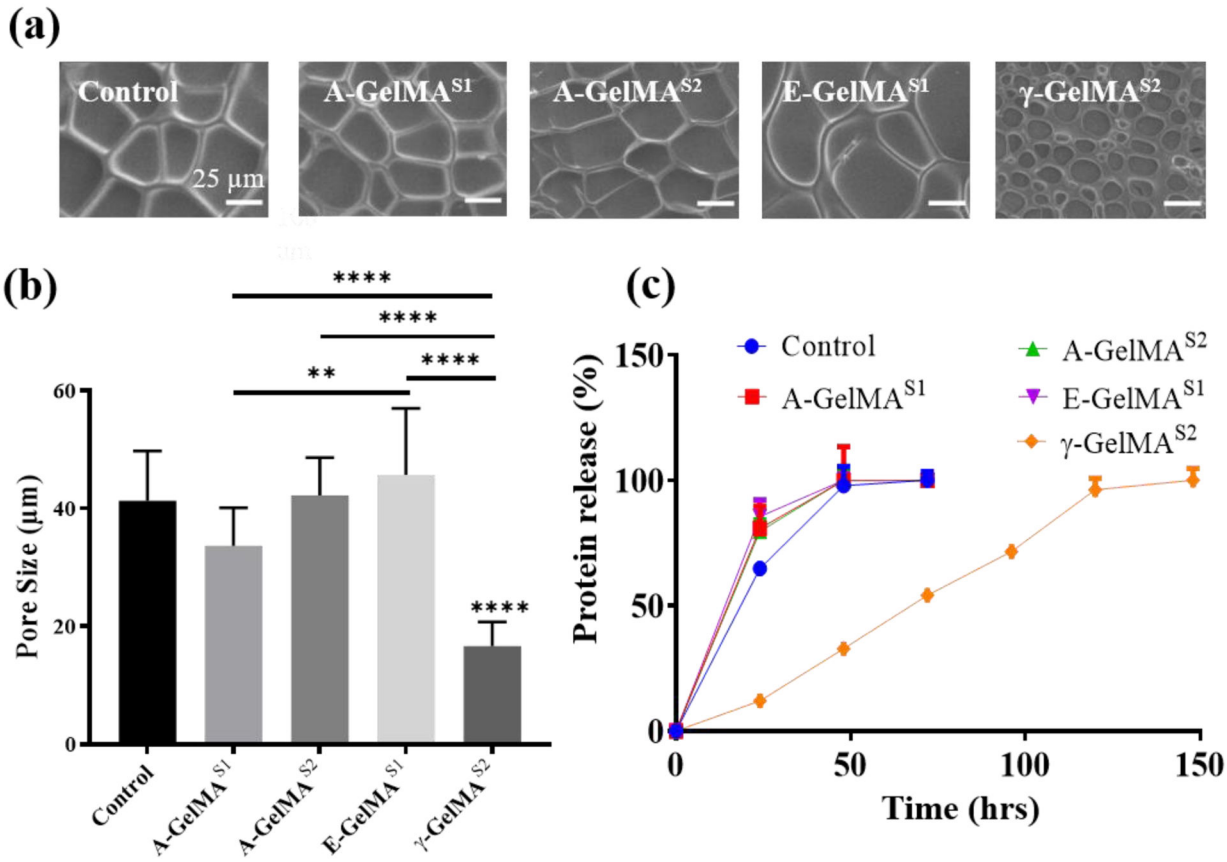

Figure 3:

(a) Representative scanning electron micrography (SEM) images of 10% freeze-dried GelMA pores. (b) Quantification of the GelMA pore size. (n=51) (c) Effect of the sterilization on the rate of enzymatic biodegradation of 10% GelMA. (n=3) * $p<0.05$; ** $p<0.01$; *** $p<0.001$; **** $p<0.0001$.

Author Manuscript Author Manuscript Author Manuscript Author Manuscript

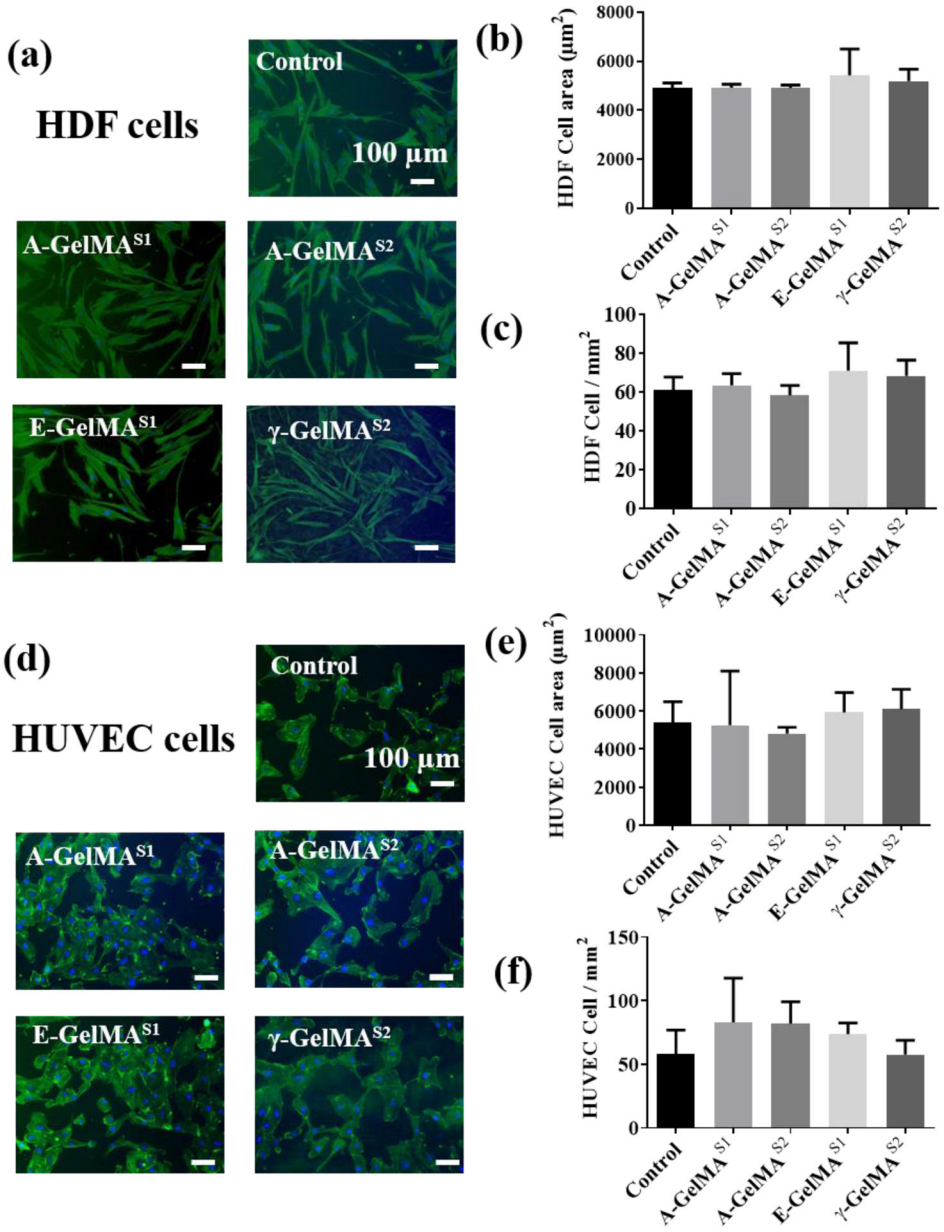

Figure 4:

Effect of Sterilization of 10% GelMA hydrogels on the human dermal fibroblasts (HDF) and HUVEC cell adhesion and spreading. (a) Representative F-actin stained HDF images on different hydrogel groups. Quantitative analysis of the effect of sterilization methods on HDF (b) cell spreading and (c) cell density. (d) Representative F-actin stained HUVEC images on different hydrogel groups. Quantitative analysis of the effect of sterilization methods on HUVEC (b) cell spreading and (c) cell density. (n=3)

Author Manuscript Author Manuscript Author Manuscript Author Manuscript

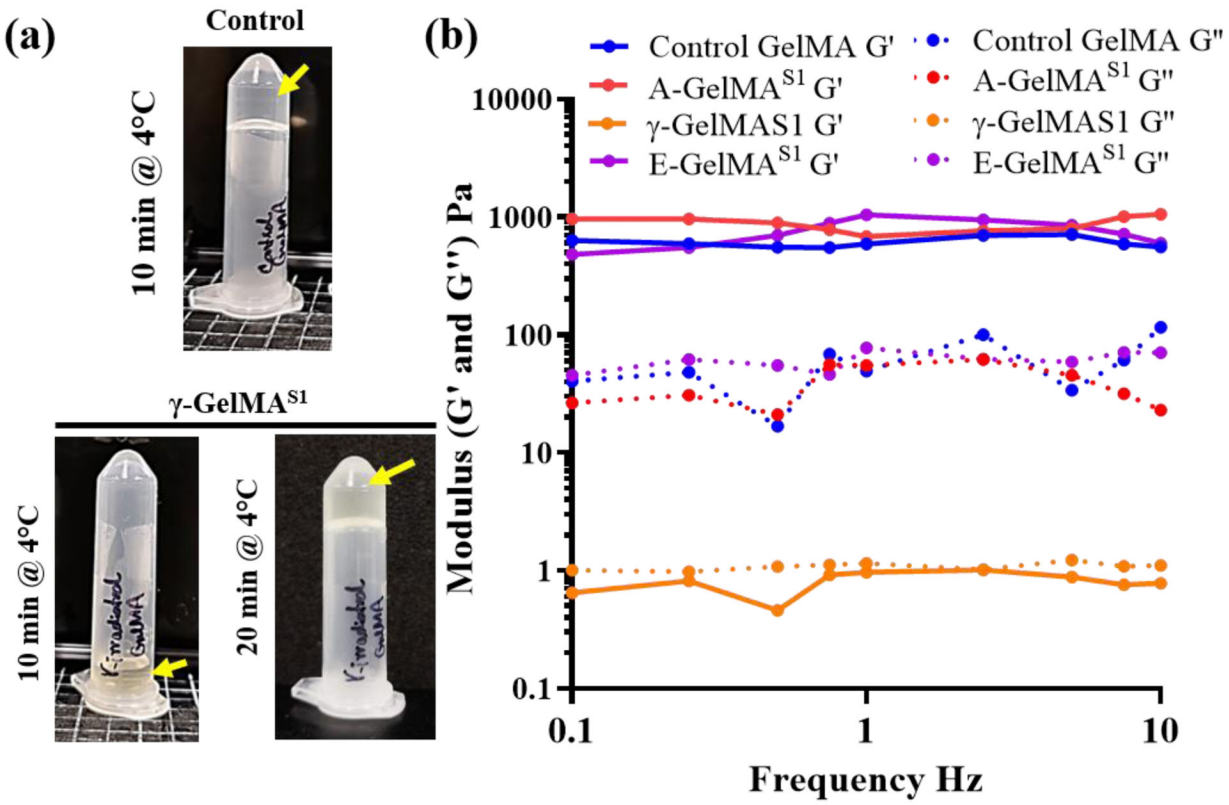

Figure 5:

Effect of sterilization treatments on 10% GelMA prepolymer solution: (a) After 10 min at 4°C, gamma irradiated GelMA did not form a physical gel and remained in solution state. However, control GelMA readily transformed to a gel state and did not flow to bottom of the vial upon inversion of the vial. (b) Storage modulus (G') and loss modulus (G") of the GelMA at different frequencies at 1% strain

Author Manuscript Author Manuscript Author Manuscript Author Manuscript

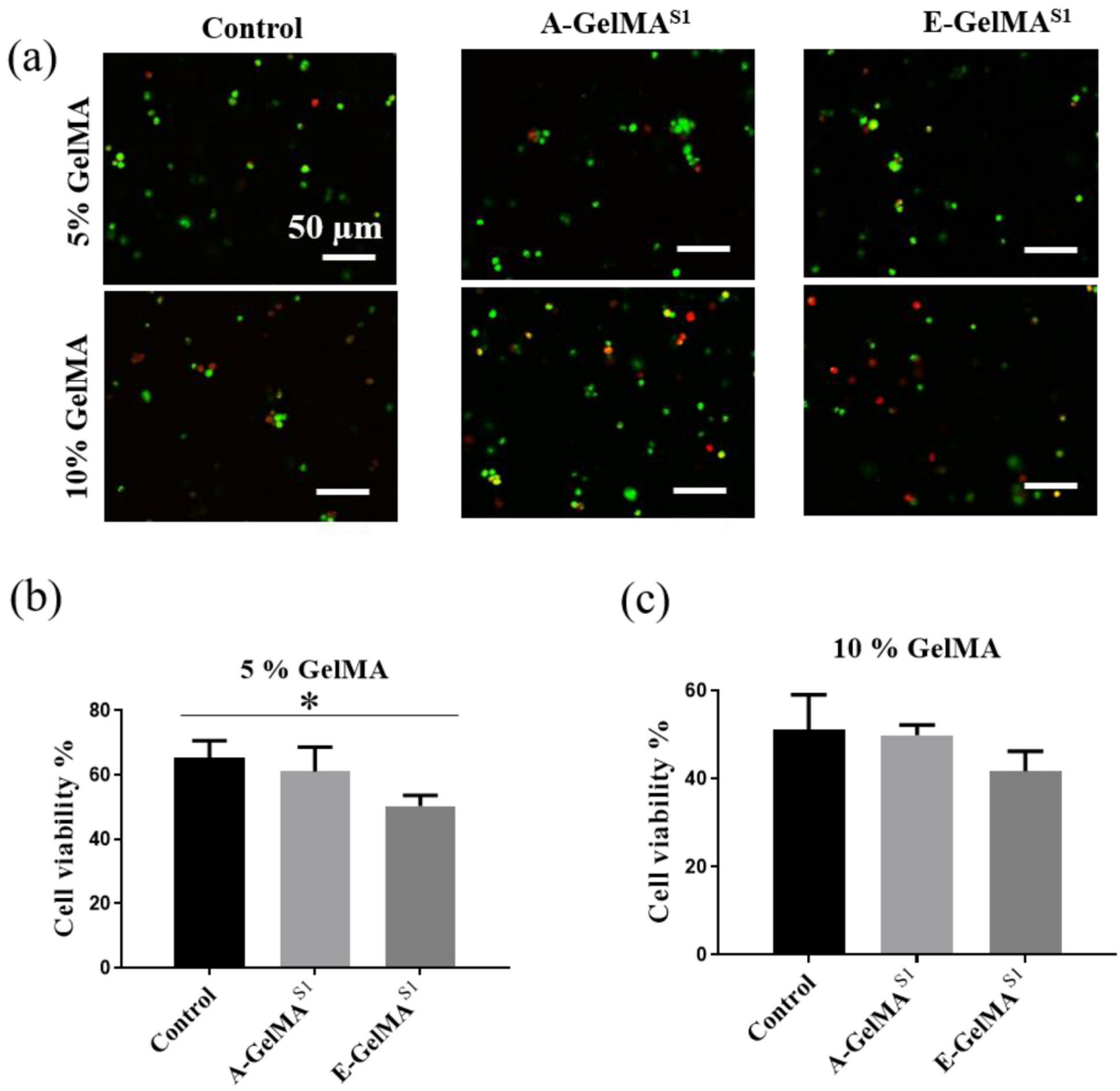

Figure 6:

Effect of Sterilization on the cell viability in 3D encapsulated cells. (a) Representative images showing the viable (green) and dead (red) cells. Quantitative analysis of the encapsulated cell viability in (b) 5% and (c) 10% GelMA hydrogels. (n=3). * $p<0.05$

Author Manuscript Author Manuscript Author Manuscript Author Manuscript

(a)

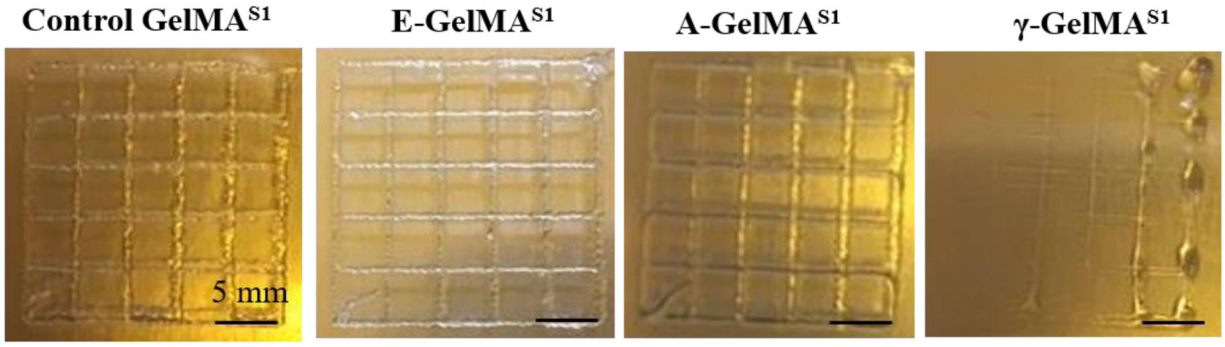

(b)

Printability			
Control GelMA^{S1}	E-GelMA^{S1}	A-GelMA^{S1}	γ-GelMA^{S1}
0.98 +/- 0.02	1.00 +/- 0.02	0.99 +/- 0.03	0.32 +/- 0.32

Figure 7:

Effect of Sterilization on the printability of the 10% GelMA bioink. (a) Representative images showing the wire grid printed structures using different sterilized GelMA bioinks. (b) Quantitative analysis of the printability ratio of the different GelMA bioinks. γ-GelMA^{S1} was found to have lowest printability of all the groups.